Polymer Manipulation and Nanofabrication in Real Time Using Transmission Electron Microscopy

R. Malcolm Brown, Jr.,*,† Zack Barnes,† Chie Sawatari,‡ and Tetsuo Kondo§

Section of Molecular Genetics and Microbiology, The University of Texas at Austin, Austin, Texas 78712, Department of Integrated Science and Technology, Shizuoka University, Japan, and Graduate School of Bioresources and Bioenvironmental Science, Kyushu University, Fukuoka 812-8581, Japan

Received June 7, 2006; Revised Manuscript Received September 14, 2006

Here we present time-resolved in situ transmission electron microscopy (TEM) observations and real-time manipulation of nematic ordered cellulose and ultradrawn polyethylene films. Drawn films of these two polymers exhibited a unique response to the low-dose electron beam. Electron beam damage was minimal based on retention of an organized electron diffraction pattern. Increased electron dosage appeared to melt the polymer with subsequent movement and attraction toward preferred electron concentrations within the beam. This discovery allowed the preferential, directed manipulation of polymer chain aggregates in two dimensions. These findings provide a basis for a new technique to manipulate and simultaneously observe dynamic assembly at the molecular level of structures using TEM.

I. Introduction

The ability to manipulate material at the nanoscale level with ion beams has proven to be invaluable in the execution of nanofabrication protocols.[1−5] Experimental manipulation and real-time observation at this scale could be vital in determining not only beginning and end products but also intermediates in the process of polymerization and polymer crystallization.[6−8] Among current nanoscale imaging and manipulative protocols, only atomic force microscopy is capable of observing the molecular structure of a variety of materials down to nanometer-level resolution on a consistent basis. It has been possible to conduct experimentation on physical phenomena such as the melting and recrystallization of polymeric specimens, with minor modifications to the device itself.[7,8] Real-time imaging, however, is virtually impossible since a relatively large period of time must be used in the actual specimen scanning to obtain the image. Additionally, focused ion beam milling, a protocol in nanomaterials fabrication that formerly was limited to semiconductors and metallic materials, has been adapted to work with soft polymers.[5,9,10]

The objective of this work is to use transmission electron microscopy (TEM) to simultaneously image, manipulate, and alter nematic ordered cellulose (NOC) and polyethylene in real time. The low electron dose and high resolution of TEM have permitted the imaging of polymer chains during specific beam manipulations that can actually control and fabricate at the nanoscale level. Such analyses with TEM heretofore have not been recognized for a variety of previously observed phenomena, and preconceived ideas regarding beam damage, thermal oxidation, free radical formation, and a host of other damaging conditions during electron irradiation have hindered progress in this field.[5,11,12] Due to the electron beam's high electronegativity, current dogma states specimens must be fixed or stained for imaging.[11,12] This is unacceptable given the demand for the construction of biocompatible nanomaterials.[13−15]

TEM analysis of polymers rarely exceeds 20K magnification of crystalline polymers for fear of localized specimen damage.[11,12] In addition, it has been well documented that the combination of the electronegativity and the collision of electrons with the specimen matrix can induce melting, pitting, and false artifacts.[11] This may be primarily related to the ion beam heating the localized specimen matrix. Electron beam damage cannot be entirely eliminated, but it can be minimized with the use of low electron dose and high sensitivity electron detection equipment. With this in mind, we sought to examine several model polymer systems for molecular imaging in real time.

We chose two very different conformational states of two linear polymer systems. The synthetic polymer studied is ultradrawn polyethylene (UDPE) with 92% crystallinity and having an orientation factor (F200) of the *c*-axis of 0.99.[16] Cellulose is a natural polymer of linear β glucose units linked 1−4. Native cellulose consists of crystalline aggregates of these glucan chains; however, we chose NOC as the preferred system because, while parallel to each other, the glucan chains are not in such high order to be crystallized. At the molecular level, NOC is not different from native cellulose; however, due to the process of dissolving the cellulose and then drying it, water has been introduced between the chains. During this drying process, the chains are H-bonded in an amorphous state. This is much like "spot welding" as the water is introduced. The water-saturated cellulose can then be linearly oriented mechanically; however, the chains do not collapse into a crystalline cellulose I or cellulose IV state. Rather, they remain oriented, yet they are not crystalline, hence the name "nematic ordered cellulose" has been given to describe this unique state of glucan chain aggregation.[17]

The arrangement of the carbon atoms in the cellulose polymer chain is a chair conformation. Each glucose monomer is linked by a glucosidic oxygen bridge. On the other hand, the linear polymer, polyethylene, consists of extended carbon* bonds. Both

* To whom correspondence and request for materials should be addressed. E-mail: rmbrown@mail.utexas.edu.
† The University of Texas at Austin.
‡ Shizuoka University.
§ Kyushu University.

10.1021/bm060546z CCC: $37.00
Published on Web 11/24/2006

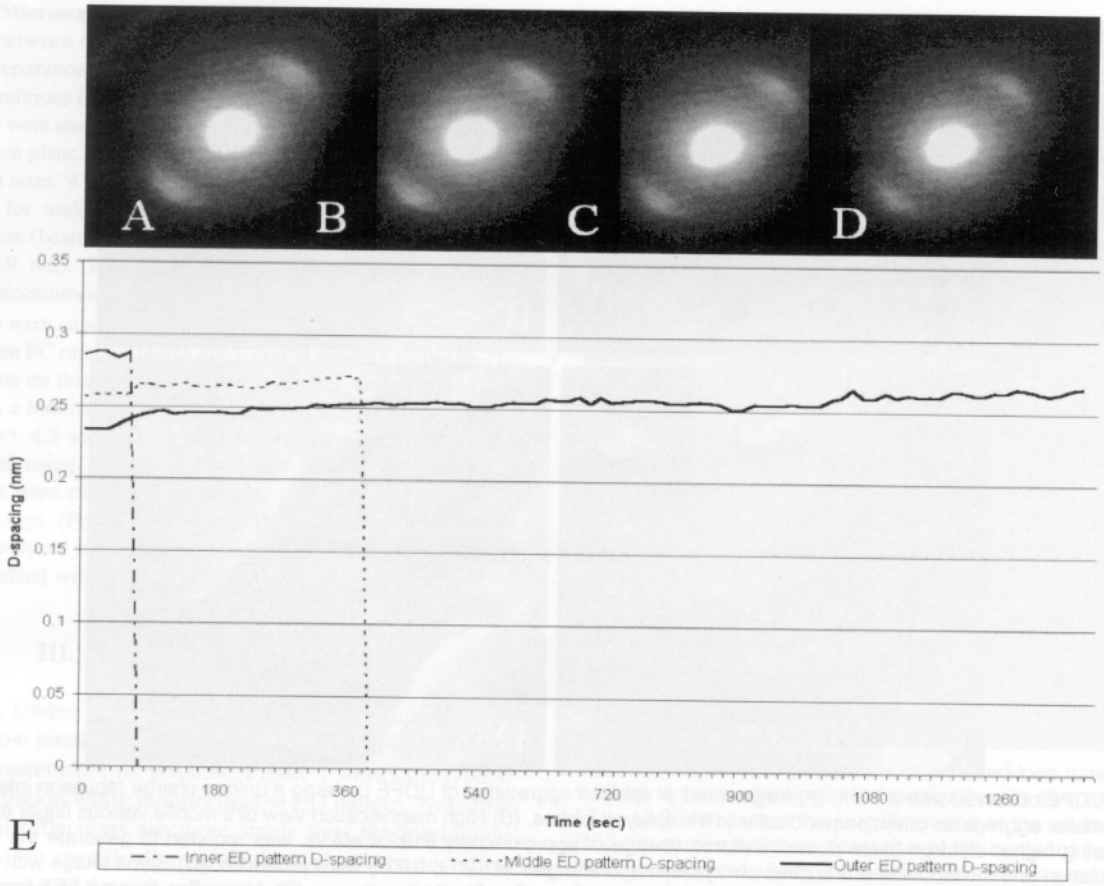

Figure 1. ED time/course analysis of UDPE d-spacings during electron irradiation. (A−D) Draw axis oriented from lower right to upper left. Equatorial reflections are shown. (A) Initial irradiation (beam spot size 6, magnification = 7.5K, accelerating voltage = 100 kV, with a beam current = 0.0025 nA, 230.7 e/Å^2/s). Note three distinct ED patterns, corresponding to d-spacings 0.2854, 0.2563, and 0.2337 nm. These d-spacings correspond with one-half of the dimensions of the 010 unit cell axis. (B) 90 s irradiation. Total irradiation is approximately 20 763 e/Å^2. (C) 405 s irradiation. Total irradiation is approximately 93 433 e/Å^2. (D) 600 s irradiation. Total irradiation is approximately 138 420 e/Å^2. (E) Graph of the d-spacings vs time.

polymers retain an amazing ability to be stretched into parallel chain arrangements. In its most relaxed state, polyethylene is chain folded, while single glucan chains are most thermodynamically stable in an antiparallel arrangement, which is most likely also to be chain folded.[18,19] Given the similarity of metastable chain-folded conditions, we wanted to examine the comparative behavior of these two different polymer systems during manipulation within the electron beam. Crystalline cellulose I is known to be sensitive to e-beam bombardment, and electron diffraction (ED) patterns rapidly degrade, even during low dose radiation.[20] Just because the ED pattern broadens and degrades upon exposure to the electron beam does not imply that the primary structure of cellulose has been destroyed. On the contrary, single glucan chains have been observed using negative staining.[17]

II. Experimental

UDPE. Uniaxially oriented polyethylene films were obtained from single-crystal gel mats crystallized from solution that were stretched to 20 000% elongation.[7] The UDPE films were cut and placed in a 3 mm grid holder of a Philips 420 TEM.

NOC. Solubilized cellulose was created by two different methods. One procedure used the mechanical disintegration of 1 g of water-swollen cotton fibers in dimethyl acetamide (DMAC). The fibrous material was then bathed in MeOH and acetone five times, before the solvent exchanged into 5% w/w LiCl/DMAC, and stirred for 21 days. The solution was centrifuged to remove insoluble material and then filtered.[17] A small amount of the solution was allowed to completely dry at room temperature to determine that the actual concentration of cellulose in the solution (wt %) was 1−4% with this method.

Another method consisted of creating solubilized cellulose via the dissolution of Sigmacell 20 micron powder in a 5% w/w LiCl/DMAC solution for 5 days. The solution was gravity filtered for 24 h under a fume hood. A small amount of the solution was allowed to completely dry at 60 °C to determine that the actual cellulose concentration of the solution (wt %) was 2−5% with this method.

The filtered solution was poured to a depth of approximately 2 mm in a 55 mm glass Petri dish and dried for 7 days at room temperature under a saturated water vapor atmosphere. This condition allowed the water vapor to diffuse into the solution, resulting in the precipitation of a gel-like, water-swollen cellulose film. The concentration of cellulose in the resultant films was found to be 7 wt % cellulose and 93 wt % water. This coincides exactly with previously reported concentrations for this protocol.[17] The gel was then cut into 50 × 10 mm strips and placed in a manual stretching device. The strips were clamped 3 mm apart and uniaxially stretched at room temperature to a length of 6.25 mm over a period of 48 h.

TEM samples were created by taking a thin diagonal section from the longitudinal side of the dried stretched gel with a razor blade. The section strip was cut to fit in the 3 mm TEM specimen holder and sandwiched between two 3 mm copper grids, a nickel folding grid, or a copper folding grid without further staining or fixative preparations.

Further TEM samples were created by the deposition of 1/20 dilution in DMAC of filtered solubilized cellulose on a vertical face of a clean glass microscope slide in a saturated atmosphere for 24 h. The slide was then horizontally dried in a saturated atmosphere for 48 h, then

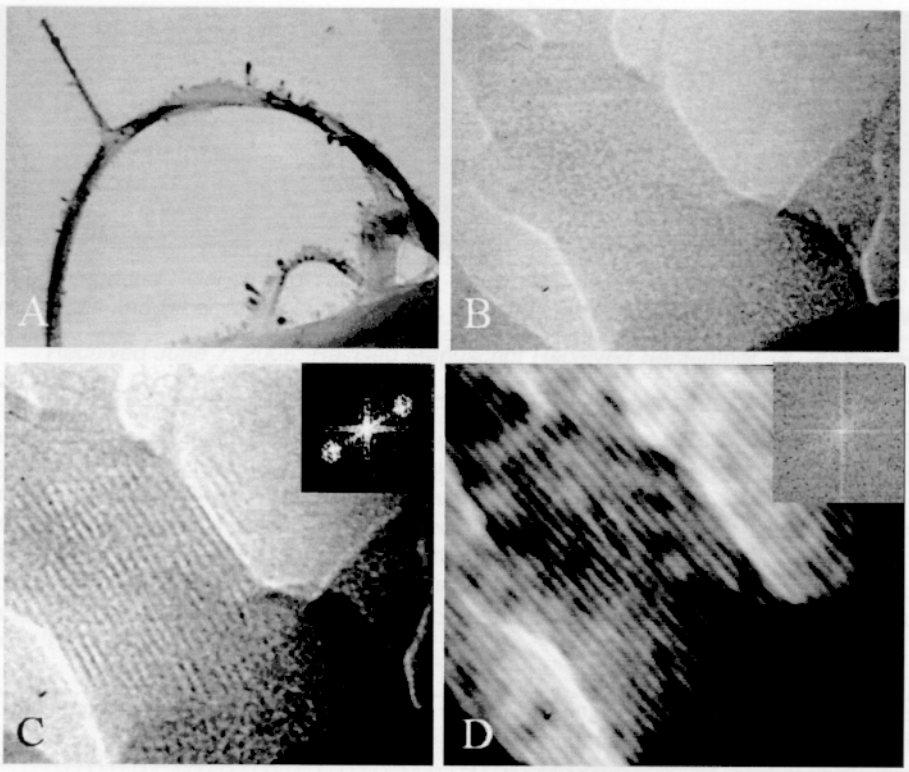

Figure 2. UDPE observed with a TEM. (A) fragmented or splayed aggregates of UDPE undergo a unique charge repulsion interaction to form "arches". Smaller aggregates orient perpendicular to the splayed arches. (B) High magnification view of a mobile viscous finger extrusion, which appears during higher electron beam doses. Electron dosage of approximately 6192.4 e/Å^2/s. was required to generate the mobile fingers. During irradiation and motion, lateral branches always with acute angles (41.9° ± 0.27°) were produced. (C) Same image with inverse FFT of selected area of interest with spike boosted regions (inset) via Image Pro Plus 4.2 software. (D) Alternative inverse FFT from Zeiss KS400 image processing software of the entire image demonstrates that the inverted wavelengths are not artifacts of the software, the FFT, or the inversion.

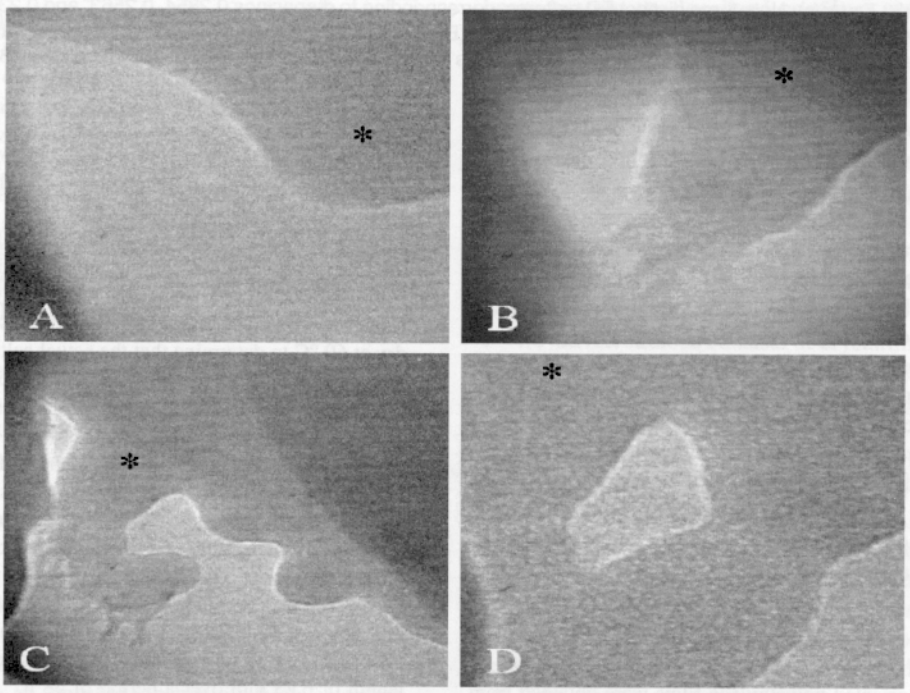

Figure 3. Sequence of electron beam manipulations during the growth of viscous fingers. The asterisk marks a fixed point from which the viscous finger grew. (A) The center of the electron beam is out of the image field at the lower left-hand corner. Initial formation of a dome occurs with its top center oriented toward the center of the electron beam. Viscous fingers always grew toward the center of the beam. (B) The 'dome' of the polyethylene extended from the upper right-hand region of the photo and extended showing dendritic chain branching and propagation. (C) The electron beam was maneuvered to form a curved 'hook' and to initiate a new dome from the original matrix toward the center of the beam. (D) Continued irradiation produced a closed loop, completing the fabrication. Magnifications of A, B, and D are the same.

air-dried under the hood at room temperature for 48 h. It was possible to slide a 3 mm copper grid under the transparent cellulose film before saturated atmosphere water vapor exchange. The film was peeled from the slide and cut to fit into the 3 mm TEM specimen holder, then sandwiched between two 3 mm copper grids, a nickel folding grid, or a copper folding grid without further staining or fixative preparations.

Electron Microscopy Conditions. In both samples, the film was sandwiched between two 3 mm copper grids without further staining or fixative preparations. Low electron dose (<250 e/Å/sec) and high-resolution conditions (>0.35 nm) were maintained at 100 kV. Specific beam settings were analyzed in situ to quantify the electron environment at the specimen plane. Beam current and diameter data were collected for beam spot sizes '4−6' on a Philips 420 TEM at 33K magnification at crossover for undersaturation, approaching saturation, and fully saturated points (beam size for spot size 4 = 68.9 nm; 5 = 45.9 nm; and 6 = 20.9 nm). The beam current was read from a Keithly autoranging picoammeter.

All images were captured with a Gatan 620 SIT camera linked to a Dell Dimension PC running Image Pro+ digital imaging software. The actual scan rate on this instrument is 30 f/sec. The analog signal was digitized with a Matrox frame grabber, and the images were digitized by Image Pro+ 4.2 software. Fast Fourier transform (FFT) analysis was conducted using Image Pro+ 4.2 and Zeiss KS400 software. Measurements were calibrated by imaging the 0.335 nm interatomic graphene spacings. (Polysciences, Inc., Warrington, PA 18976). The images were analyzed via platforms Zeiss KS 400 and Adobe Photoshop Pro and assembled with Paintshop Pro.

III. Results and Discussion

A. UDPE. Under low dose imaging, relatively thin margins of UDPE allow transmission of the electron beam so that real-time ED measurements are possible. Figure 1 shows the typical result of irradiation while monitoring the ED pattern. Note that the equatorial reflections are more stable than the meridional reflections. More specifically, the analysis shows preservation of the *b* dimension of the unit cell where the outermost reflection remains relatively unchanged over more than 1200 s of electron beam irradiation (Figure 1A−D). This represents more than 276 840 e/Å^2. The preservation of a semicrystalline structure with a high total dose is due to the sample tolerating 237e/Å^2/s. This may be sufficiently low to minimize damage to the polymer structure. These new data shed light on the interaction between the electron beam and molecular preservation, namely, that under relatively low electron beam dosages (~300 e/Å^2), the sample can be sufficiently protected against gross beam damage during continued exposure.[5,9,10] This may imply that manipulation of the electron beam can be used to analyze soft polymers for extended electron irradiation, similar to protocols used in focused ion beam milling.[5,9,10]

The extended duration of the equatorial reflections implies that the polymer chains do not significantly change in their distance from one other during electron irradiation. The loss of meridional reflections with the conservation of equatorial reflections implies that distance between atoms along the molecular chain is rendered dynamic by the interaction with the electron beam. This may be a result of two situations, the first being a movement of individual or groups of polymer chains, parallel to the axis of orientation. The second possibility would be that the electron beam is causing each single chain to vibrate. It is our hypothesis that both of these possibilities may play a role in the capacity for manipulation.

The thin margin, namely, the edge of the UDPE, allows electrons to be transmitted and thus diffracted, revealing much about the nature of the irradiation process not only in the ED mode but also directly by the imaging mode. In addition to the ED patterns described above, the samples tend to show a possible surface charge−repulsion through the splaying of aggregates of polyethylene (Figure 2A). We hypothesize that during irradiation, free radicals are produced on the polymer surface. The core regions maintain their relatively undisturbed

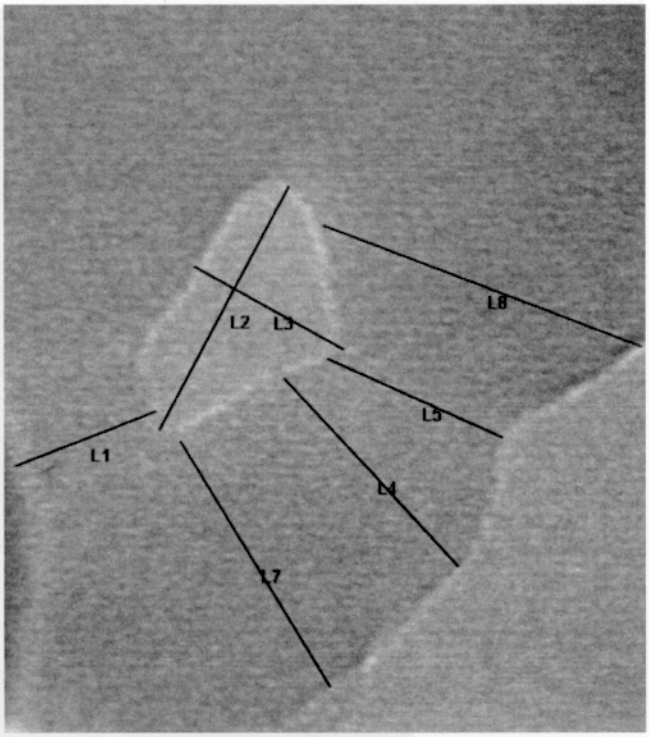

Figure 4. Measured dimensions of a closed-loop nanoring: L1 = 8.03 nm to the overlapping fold of the significantly thin polymer matrix; L2 = 15.30 nm across the long dimension of the center hole; L3 = 8.63 nm across the short dimension of the center of the ring; L4 = 13.53 nm; L5 = 10.10 nm at the fusion point; L6 was out of the image frame and discarded; L7 = 16.04 nm; and L8 = 16.49 nm across the bases of the final extension closure.

crystalline structure (as evidenced by ED, not shown). Often, the aggregates form at right angles to the surface of the stretched polyethylene sheet, suggesting that a charge repulsion is being neutralized perpendicular to the sheet axis. This is further supported by perpendicular subaggregates that split from curved surfaces of earlier splayed aggregates (Figure 2A).

When a charge repulsion occurs in conjunction with a semifluid state, a more complicated interaction is observed. Higher electron beam doses appear to 'melt' the polymer chain aggregates while maintaining molecular chain orientation, and the polymer chains move in predictable directions from the UDPE surface. Figure 2B shows a viscous finger formed within a few seconds exposure to the electron beam. This extension always propagates toward the center of the electron beam and produces branches that are consistently oriented less than 90 degrees. Videos are available to demonstrate these propagations in real time (Supporting Information). Low-dose TEM of the structures at the tip of a growing viscous finger reveals single polyethylene polymer chains migrating from the surface, followed by movements of multiple polymer chain aggregates. We hypothesize that, as the sample is sufficiently heated and charged, the charge repulsion interaction loosens the matrix constraints, allowing propagation toward the center region of the electron beam. A single-pixel gray value trace of electron intensity across the beam (data not shown) confirms the Gaussian distribution of electrons.[5] The total net charge within the beam is greatest at its center. Thus, the beam intensity may induce the attraction of the oppositely charged free radicals on the polymer surfaces. The result is directed movement of the polyethylene toward the center of the beam due to the positive free radical introduction on the polymer surface.

During viscous finger formation, multiple polymer chains appear to migrate parallel to each other *en masse*, maintaining

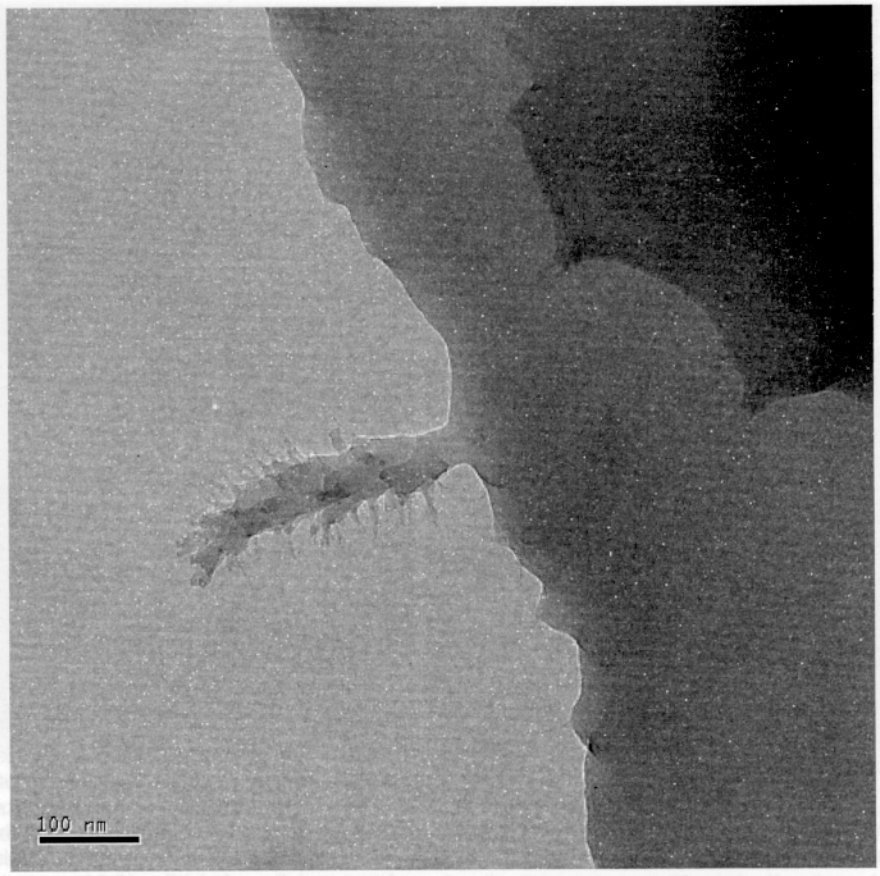

Figure 5. NOC film made from the thin edge of stretched gel. Single primary viscous finger extension showing some secondary branching. Image taken with beam spread; original extrusion taken at 100 kV, 0.0879 nA beam current.

a nematic order as shown by FFT analyses in Figure 2C,D. If the viscous fingers maintain nematic order during electron irradiation, the charge repulsion hypothesis still sufficiently explains this observation. A lower interaction in this case may imply individual polymer chains are sufficiently charged via charge formation so that they maintain aggregation but lack crystalline order. This would allow for directed chain motion created by the net charge with the electron beam. Thus, the FFT analysis verifies parallel molecular order within the viscous fingers during their motion in the electron beam.

Viscous finger branching can also be explained in terms of the charge−repulsion hypothesis and interaction with the electron beam. The tip of the propagation always orients toward the center of the electron beam, and the normal progression of events is the emergence of a 'burst' of small chain aggregates from the surface. If small polymer aggregate chains have sufficient charge, they repel each other at their tips, but they are still anchored within the mass of oriented chains. The mutual repulsion creates an acute angle that becomes stabilized during the multiple migrations of small chain aggregates to form the nematically ordered viscous finger (Figure 3). Charging and heating of the sample appear to drive these nanoscale propagations.

Real-time video data of the propagation and branching of these viscous fingers and small aggregates are available online (Supporting Information). These videos demonstrate the initial few lead aggregates as they begin extending into preferred electron densities within the beam, and then begin recruiting, probably through interchain associations, an increasing number of other molecules, ultimately increasing the mass of the polymer propagating into the beam. This increase in mass and the fine control of the quantity of molecules in motion may lead to a precision control of these viscous fingers. Such control would be vital in determining the size, shape, quantity, and possibly the molecular weight of the polymer chains moving into and interacting with the electron beam during nanofabrication.

B. NOC. The phenomenon found in UDPE has also been investigated with biopolymers, exemplified with a special form of cellulose known as NOC. The properties of NOC exist such that the glucan chains are not tightly ordered, but directionally oriented.[17] This did not allow for the same long-term low-dose ED as that used in UDPE, as it would be impossible to obtain a useful or meaningful ED pattern. Furthermore, this characteristic did not show the same thin edge splaying that was observed in UDPE. UDPE with highly oriented and tightly interacting chains is, again, not present in the NOC.

In contrast with polyethylene, NOC is not a crystalline system, yet it maintains an order. It was primarily observed that the beam partially melted the thin edges of the polymer and led to viscous finger-like extensions. In the NOC, however, the required electron dosage was an order of magnitude lower than that required for manipulative studies in UDPE. This lower energy requirement its thought to be related to the fact that the nematic ordered state is less energetically linked than a completely crystalline structure. However, it is found that NOC behaves very similarly to the UDPE in aggregate propagation and capacity for manipulation.

The viscous finger propagation begins with a localized swelling of the melted polymer after a short period of irradiation usually lasting a few seconds, with the electron beam at a significantly thin edge of the polymer. Then individual chains or small aggregations of polymers splay from the swelling and begin a fluidic extension into specific areas within the beam.

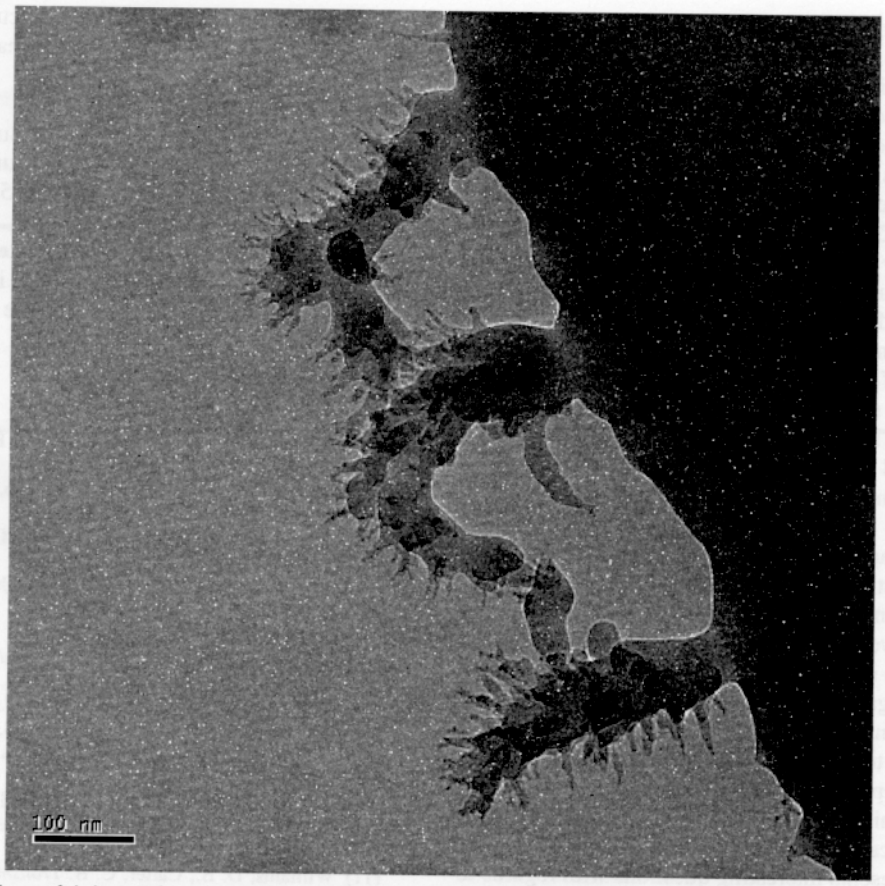

Figure 6. Closed serial loops fabricated from the NOC polymer edge demonstrating the repeatability of structural formation and the proximity of the manipulative experiment.

The ends of these chains are believed to be the result of damage to the specimen, particularly where an electron has been removed from the molecule as a result of a collision with an electron in the beam. The result of such knock-out damage could be the production of a free radical that has localized to the break. The core portion of the polymer is thought to have remained unaffected. The angle of the secondary extensions that move into the beam has been found to be conserved at $44.09 \pm 18°$. While there is a broad range of angles observed, this shows that, for the most part, the angles are acute. This again is hypothesized because of the charge−repulsion from the free radicals at the tip of the semifluid extensions and the induced dipole covering the surface of the main polymer matrix. The resolution of antagonistic effects would result in an angle that would equilibrate the angles from the main polymer matrix and from the body of the initial polymer extension.

These extensions can be manipulated by location of the beam. In Figure 5, a single viscous finger propagation is drawn to a length exceeding 300 nm. The frequent branching points are approximately 20 nm in width. At this large scale, the polymer chain aggregates can be manipulated and directed by the user. Figure 6 shows a series of extensions that were manipulated by the e-beam into curve linear shapes, in this case forming an 'M'. The only drawback to this technique is that it must be done in series, and therefore the time between manipulations and end products may be excessive for commercial purposes. Applications already conducted via focused ion beam techniques may be conducted with this instrument.

Bond energies across the surface of polymeric systems show that hydrogen bonds, like those found in polyethylene and more so in cellulose films, have a bond energy of approximately 3−7 kcal/mol, while van der Waals attractions typically only range from 1 to 2 kcal/mol. For this reason, it is hypothesized that the lower beam current created by the smaller beam is sufficient to allow manipulations in the NOC, which does not have the tight hydrogen bonds and van der Waals forces associated with a high percent crystalline cellulose, similar to what is found in highly crystalline UDPE. Since NOC is not highly crystalline, the interactions between individual glucan chains forms a considerably looser matrix. This loose association between the polymer chains means that less energy is required to manipulate the polymer aggregates once a free radical has been formed near a chain scission point. Since we hypothesize that a free radical is formed by such a break in an individual or multiple chains, it is the amount of energy required to do this that is dependent on the number of stabilizing interactions or associations between the broken chain with its free radical and the chains adjacent to it within the matrix.

By demonstrating that this protocol is feasible for two diverse polymeric systems, it may be reasonable to conclude that it is possible for other polymer systems to be similarly manipulated. The implementation of this type of focused ion beam manipulation may have further implications in the growth and development of new protocols in nanotechnology. Of particular note is that this interaction takes place at a beam energy far lower than that which is used for other purposes, such as ion beam milling. Advancement in this technology may have other future possibilities beyond the two selected polymeric systems.

C. Future Directions. This research implicates a novel protocol for low-dose, low-beam current TEM. This would allow real-time manipulation and imaging of manipulative experiments in materials formerly considered too fragile to be examined and studied in a TEM environment. Current research and development in novel imprinting, ion beam lithography, and pattern

transfer techniques may be impacted by the use of similar protocols for using soft polymeric systems. It may be possible to enhance the resolution during propagation of these structures using photo- or electroresists created by other techniques. The protocols presented here show the potential for top-down and bottom-up techniques to be applied in the synthesis of novel meso- and nanoscale structures. Further protocols for the development of masks or substrates for other building blocks in nanomaterials may be possible as well.

Technological advances in specimen holder technology and the growth of the field of in situ TEM technologies may further enhance the development of these protocols. Particularly applicable is the use of controllable manipulative actuators and plates that can apply strains, stresses, and shears to polymeric samples while they are being observed. Further, using the electron beam would advance the capabilities of the TEM in the research environment. It may be possible to determine how many systems react to the ion beam structurally as when mechanical stresses are simultaneously being applied.

Use of the newest generation TEM holders may also be possible to fabricate masks for various lithographic and imprinting procedures that were not previously possible. Additionally, it may be possible to synthesize these resists out of previously unexplored or disregarded materials for both top-down and bottom-up fabrication techniques.

This manipulative technique, while still in its infancy, shows an interesting dual capability for TEM, and, using a biopolymer such as cellulose, this approach introduces a whole field of materials not historically explored for nanomaterials research. Additionally, this presents interesting questions with regards to other biological materials that may be used for nanofabrication. The possibility of DNA, RNA, extended proteins, or other biological polymers being used for nanotechnology is another area of future exploration. It may become possible to use the semi-melting character of soft polymers to 'weld' other substrates or similar polymers at a joint. Similar to welding, this approach may allow the construction of hybrid systems, with two different polymer sheets joined in such a fashion at the nanoscale to be used as substrates for different purposes. This could be used to draw the polymer to create a bridge between two other molecules, resists, or masks for purposes such as building capacitors or electron bridges with other materials. The potential of this protocol is only limited by the time required to produce and propagate multiple structures in series. In time, that may also be overcome with automation and multiple beam arrays.

Acknowledgment. This work was supported in part by Grant F-1217 to R.M.B. from the Welch Foundation and the Department of Energy DE-FG03-94ER20145.

Supporting Information Available. Four movies demonstrating the real-time motion of UDPE imaged and manipulated in a TEM. This material is available free of charge via the Internet at http://pubs.acs.org.

References and Notes

(1) Senaratne, W.; Andruzzi, L.; Ober, C. K. *Biomacromolecules* **2005**, *6* (5), 2427−48.
(2) Ye, Q.; Cassell, A. M.; Liu, H.; Chao, K.-J.; Han, J.; Meyyappan, M. *Nano Lett.* **2004**, *4* (7), 1301−8.
(3) Sivanesan, P.; Okamoto, K.; English, D.; Lee, C. S.; DeVoe, D. L. *Anal. Chem.* **2005**, *77* (7), 2252−8.
(4) Poggi, M. A.; Bottomley, L. A.; Lillehei, P. T. *Anal. Chem.* **2002**, *74* (12), 2851−62.
(5) Gates, B. D.; Xu, Q.; Stewart, M.; Ryan, D.; Willson, C. G.; Whitesides, G. M. *Chem. Rev.* **2005**, *105* (4), 1171−96.
(6) Brown, B. A.; Brown. *Am. Lab.* **2001**, *33*, 13−20.
(7) Ashkin, A. *Proc. Natl. Acad. Sci. U.S.A.* **1997**, *94*, 4853−60.
(8) Pearce, R. Vansco, G. *J. Polym.* **1998**, *39* (5), 1237−42.
(9) Hobbs, J. K.; Humphris, A. D. L.; Miles, M. *J. Macromolecules* **2001**, *34*, 5508−19.
(10) Niihara, K.; Kaneko, T.; Suzuki, T.; Sato, Y.; Nishioka, H.; Nishikawa, Y.; Nishi, T.; Jinnai, H. *Macromolecules* **2005**, *38*, 3048−51.
(11) Williams, D. B.; Carter, C. B. *Transmission Electron Microscopy: A Textbook for Materials Science*; Plenum Press: New York, 1996; Vols. 1−4.
(12) Peacock, A. J. *Handbook of Polyethylene: Structures, Properties and Applications*; Marcel Dekker, Inc.: New York, 2000.
(13) Shenhar, R.; Rotello, V. M. *Acc. Chem. Res.* **2003**, *36* (7), 549−61.
(14) Gourley, P. L. *Biotechnol. Prog.* **2005**, *21* (1), 2−10.
(15) Rosi, N. L.; Mirkin, C. A. *Chem. Rev.* **2005**, *105* (4), 1547−62.
(16) Sawatari, C.; Matsuo, M. *Macromolecules* **1986**, *19*, 2036−40.
(17) Kondo, T.; Togawa, E.; Brown, R. M., Jr. *Biomacromolecules* **2001**, *2*, 1324−30.
(18) Kolpak, F. J.; Blackwell, J. *Macromolecules* **1976**, *9*, 273−8.
(19) Stipanovic, A. J.; Sarko A. *Macromolecules* **1976**, *9*, 851−7.
(20) Morin, F. G.; Jordan, B. D.; Marchessault, R. H. *Macromolecules* **2004**, *37*, 2668−70.

BM060546Z